

## A comparison of the distribution of necrotic core in bifurcation and non-bifurcation coronary lesions: an *in vivo* assessment using intravascular ultrasound radiofrequency data analysis

Héctor M. García-García<sup>1\*</sup>, MD, MSc, PhD; Josep Gomez-Lara<sup>1</sup>, MD; Nieves Gonzalo<sup>1</sup>, MD; Scot Garg<sup>1</sup>, MB, ChB, MRCP; Eun Seok Shin<sup>1</sup>, MD, PhD; Dick Goedhart<sup>2</sup>, PhD; Patrick W. Serruys<sup>1</sup>, MD, PhD

1. Thoraxcenter, Erasmus Medical Center, Rotterdam, The Netherlands; 2. Cardialysis, Rotterdam, The Netherlands

The authors have no conflict of interest to declare.

### KEYWORDS

Necrotic core, intravascular ultrasound, coronary arteries, bifurcation lesions

### Abstract

**Aims:** High-risk plaques are prone to develop at the site of coronary vessel bifurcations. The distribution of necrotic core at bifurcation lesions (BL) is known, however, little has been described on the necrotic core distribution in non-BLs. Therefore we compared the distribution of necrotic core between BL and non-BLs in coronary arteries using IVUS-VH imaging.

**Methods and results:** A total of 129 patients (112 non-BL and 108 BL) were included. The lesions were divided into upstream and downstream segments according to the location of the minimum lumen area (MLA) within the plaque. In BLs, compositional analysis showed no differences between the three segments. The necrotic core in contact with the lumen that was located in the downstream segment was significantly larger. While in non-BLs, this was not significantly different between segments. Plaque burden in BLs was  $56.60 \pm 5.79\%$  vs.  $55.50 \pm 4.54\%$  in non-BLs,  $p=0.04$ . Mean necrotic core area was larger in BLs  $0.84 \pm 0.55 \text{ mm}^2$  vs.  $0.70 \pm 0.49 \text{ mm}^2$ ,  $p=0.048$ . Mean percentage necrotic core was  $15.48 \pm 8.02\%$  vs.  $14.51 \pm 7.64\%$ ,  $p=0.37$ . There was a trend towards a greater content of necrotic core in contact with the lumen in BLs. The percentage of frames with a major confluent pool of necrotic core in contact with the lumen  $>10\%$  in BLs was  $11.78 \pm 17.18$  vs.  $8.95 \pm 17.86$  in non-BLs,  $p=0.065$ . There was a statistically significant difference in the frequency of IVUS derived thin capped fibroatheromas between bifurcation lesions 20 vs. 13 in non-bifurcation lesions,  $p=0.03$ .

**Conclusions:** Bifurcation lesions appear to have a larger plaque burden with a different plaque composition compared to non-bifurcation lesions. This may partly explain the adverse outcomes seen following treatment of bifurcation lesions in contemporary practice.

\* Corresponding author: Thoraxcenter, Z120, Dr. Molewaterplein 40, 3015-GD Rotterdam, The Netherlands

E-mail: h.garciagarcia@erasmusmc.nl

## Introduction

Atherosclerotic plaque is the pathognomonic characteristic of the early stages of atherothrombosis, the final consequence of vascular inflammation, cholesterol deposition and thrombus formation. The identification of sub-clinical high-risk plaques (i.e., necrotic core rich plaques) using intra-vascular ultrasound-virtual histology (IVUS-VH) is potentially important because these plaques may have a greater likelihood of rupture and subsequent thrombosis.<sup>1</sup> Studies indicate that these high-risk plaques are prone to develop at the site of coronary vessel bifurcations due to the specific shear stress conditions present in these regions. For example an *in vivo* study of 103 bifurcations, using IVUS-VH and optical coherence tomography, found that the per cent of necrotic core at the proximal rim, bifurcation and distal rim was 16.8%, 15.2% and 13.5%, respectively ( $p < 0.001$ ). Contrary to this, little is presently known about the necrotic core distribution in non-bifurcation lesions.<sup>2</sup> Therefore we compared the distribution of necrotic core between bifurcation and non-bifurcations in coronary arteries using IVUS-VH imaging.

## Material and methods

### Patient selection

The Volcano Registry is a global, prospective, multi-centre (42 centres), non-randomised study that started in March 2004, and enrolled 990 patients with coronary artery disease who had IVUS-VH performed during coronary catheterisation. For this substudy, all patients were screened for eligibility: presence of a side branch ( $> 1.5$  mm in diameter) within the imaged segment. Eventually 129 patients were selected who were older than 18-years of age. The local ethical committee of each participating centre approved the protocol and informed written consent was obtained from all patients.

### IVUS-VH acquisition and analysis

Imaging acquisition was performed during invasive coronary angiography either during diagnostic procedures, or in the non-culprit vessel during percutaneous coronary intervention (PCI).

Briefly, IVUS-VH uses spectral analysis of IVUS radiofrequency data to build tissue maps that are correlated with a specific spectrum of the radiofrequency signal and assigned colour codes (fibrous [labelled green], fibrofatty [labelled greenish-yellow], necrotic core [labelled red] and calcium [labelled white]).<sup>5</sup>

In the Volcano Registry IVUS-VH data was acquired using the Eagle-Eye™ 20 MHz catheter, (Volcano Therapeutics, Rancho Cordova, CA, USA) and a continuous pullback by a dedicated IVUS-VH console (Volcano Therapeutics, Rancho Cordova, CA, USA). The IVUS-VH data were then stored on a DVD and sent to an independent Corelab (Cardialysis, Rotterdam, The Netherlands) for offline analysis. Data acquisition was ECG-gated and recorded during the automated withdrawal of the catheter using a mechanical pullback device (TrakBack II/R-100 Volcano Therapeutics, Rancho Cordova, CA, USA) at a pullback speed of 0.5 mm/s. Geometrical and compositional data were obtained for every slice. The contours of the external elastic membrane (EEM) and the lumen-intima interface enclosed an area that was defined as the coronary plaque plus media area. Plaque burden was defined as  $([EEM_{area} - Lumen_{area}] / EEM_{area}) \times 100$ . Direct measurements (lumen and vessel cross-sectional areas – [CSA]) were also determined. Quantification of the necrotic core in contact with the lumen was performed using MATLAB® (MathWorks, Natick, MA, USA).

### Bifurcation lesions analysis

All consecutive frames with a plaque burden  $\geq 40\%$  around a side branch  $\geq 1.5$  mm in diameter were considered part of the lesion. This lesion was divided into upstream and downstream segments according to the location of the minimum lumen area (MLA) within the plaque. Imaging was only performed in the main branch (Figure 1).

### Non-bifurcation lesion analysis

These lesions were defined as follows: all consecutive frames with plaque burden  $\geq 40\%$  were considered as part of the non-bifurcation lesion. Lesions in the same coronary segment were required to be at least 5 mm apart to be considered separately.

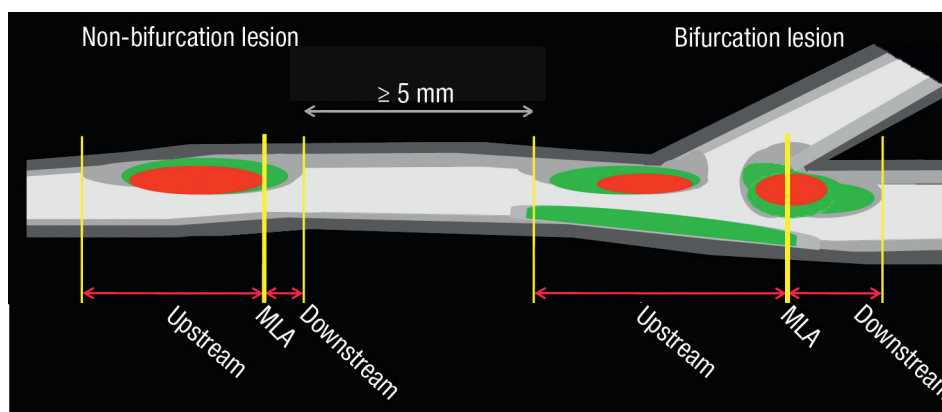


Figure 1. The bifurcation and non-bifurcation coronary lesions assessed in this study. The lesions were divided into three sub-segments: Upstream, minimum luminal area (MLA) and downstream sub-segments. Please note that the lesions should be more than 5 mm apart from each other.

Within these lesions, the frame with the MLA was selected as the divider of the plaque, that is the plaque was divided into the upstream (proximal to the MLA) frame and the downstream segments (distal to the MLA) frame (Figure 1).

In general, only lesions that have upstream and downstream frames were included for the comparison between these two segments.

## Definitions

Necrotic core tissue in contact with the lumen (NCCL), defined as the presence of necrotic core tissue in direct contact with the luminal space and with no detectable overlying fibrous tissue; it was reported (i) as percent of the total plaque composition and (ii) as a percent of the total necrotic core. In addition, the major confluent pool of NCCL (MCNC) was selectively quantified as a percentage of both the total plaque composition and the total necrotic core (Figure 2).<sup>3,4</sup>

IVUS-derived TCFA (IDTCFA), defined as a lesion fulfilling the following criteria in at least three consecutive CSAs : (i) plaque burden  $\geq 40\%$ ; (ii) confluent necrotic core  $\geq 10\%$  in direct contact with the lumen in the investigated CSA (Figure 2); all consecutive frames having the same morphologic characteristics were considered as part of the same IDTCFA lesion.

The percentage of frames per lesion having more than 10% MCNC in contact with the lumen was calculated as follows: number of frames in the lesion with  $>10\%$  MCNC in contact with the lumen divided by their counterparts X 100.

## Statistical analysis

Discrete variables are presented as counts and percentages. Continuous variables are presented as means  $\pm$  1 standard deviation. The distribution of the different variables were tested with Kolmogorov-Smirnov and in case of non-normal distribution non-parametric statistics were used to calculate p values for the comparison between two groups.

The bifurcation and non-bifurcation (lesions) were the units of analysis without corrections for correlated observations in the same subjects.

A two-sided P value  $<0.05$  was required for statistical significance. All analyses were performed using SPSS version 15.0 software (SPSS Inc., Chicago, IL, USA).

## Results

A total of 129 patients (112 non-bifurcation lesions and 108 bifurcation lesions) were included. The baseline characteristics of the patient population are shown in Table 1. The mean age was  $62.6 \pm 11.2$  years, most being male patients (78.3 %). The vessel of interest was the left anterior descending (LAD) in 48.1%, the left circumflex (LCX) in 20.1% and the right coronary artery (RCA) in 31.8% patients. Patients presented with stable angina 65.5% and 23.8% had non-ST segment elevation acute coronary syndrome.

**Table 1. Baseline patients characteristics.**

n=129	N (%)
Age (years); Mean (SD)	62.6 (11.2)
Females	28 (21.7)
Hypertension	80 (62.0)
Hypercholesterolaemia	71 (55.0)
Diabetes mellitus	28 (21.7)
Smokers	37 (28.7)
Family history of CHD	56 (43.4)
Prior history of CHD	74 (57.4)
Clinical presentation:	
Stable angina	80 (65.5)
Non-ST-ACS	29 (23.8)
ST-ACS	13 (10.7)
Study vessel:	
LAD	62 (48.1)
LCX	26 (20.1)
RCA	41 (31.8)
Pullback length, mm. Mean (SD)	48.5 (18.0)

SD: standard deviation; CHD: coronary heart disease; Non-ST-ACS: Non-ST elevation acute coronary syndrome; ST-ACS: ST elevation acute coronary syndrome; LAD: left anterior descending; LCX: left circumflex; RCA: right coronary artery

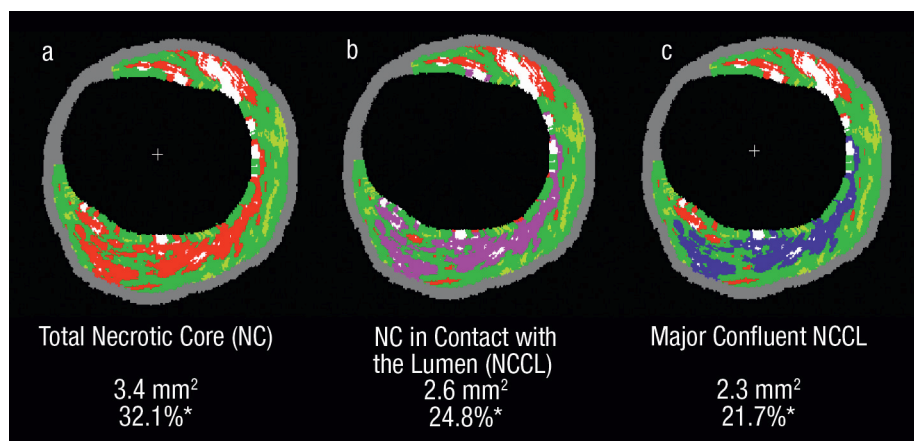


**Figure 2.** This figure illustrates the detailed quantification of the necrotic core that is in contact with the lumen. a) Total necrotic core is in red; b) Necrotic core in contact with the lumen is in violet; c) Major confluent necrotic core in contact with the lumen is in blue. \*%necrotic core of plaque area

The locations of the bifurcation lesions were as follows: LAD/Diagonal=39, LAD/septal=12, LCX/1st obtuse marginal (OM)=17, LCX/2nd OM=3, RCA/ventricular branch=14, RCA/posterolateral=5.

### IVUS-VH findings in bifurcation lesions

In Table 2, the geometrical and composition analyses are shown of the 90 bifurcation lesions which had upstream and downstream frames. The overall mean length of the bifurcation lesions was 14.62±14.24 mm, whilst the upstream and downstream segment lengths were 9.09±11.90 mm and 5.03±3.00 mm, respectively. As expected, the MLA frame had the largest plaque burden as compared to the other two segments (p<0.001). The vessel CSA at the MLA frame was smaller than the other segments (p<0.001), which was largely due to the location of the MLA frames with respect to the side branch (25.3% of the MLA frames were located proximal to the side branch of the bifurcation, 21.8% at the side-branch site and 52.9% distally).

Overall, the relative compositional analysis showed no differences between the three segments. Specifically, only the necrotic core in contact with the lumen that was located in the downstream segment was significant.

A total 20 ID-TCFAs were found in these 90 bifurcation lesions. Five of them involved upstream as well as downstream segments, whilst among the remaining, eight were located upstream and seven downstream (p=0.9).

### IVUS-VH findings in non-bifurcation lesions

Out of 112 non-bifurcation lesions, 95 had upstream and downstream frames. The geometrical and composition analyses are shown in Table 3. The overall mean length of the non-bifurcation

lesions was 9.84±9.65mm, whilst the upstream and downstream segments measured 5.47±7.66mm and 3.88±5.97mm respectively.

Similarly to bifurcation lesions, the MLA frame had the largest plaque burden as compared to the other two segments (p<0.001). Interestingly, the vessel CSA at the MLA frame was smaller than the other segments which may imply constrictive remodelling in this part of the plaque (p=0.011). Again the compositional analysis showed no differences between the three segments. Of note, although not significant, the amount of necrotic was larger in the upstream segment and the MLA, as compared to the downstream segment.

The necrotic core in contact with the lumen was not significantly different between the three segments. A total 13 ID-TCFAs were found in these 95 non-bifurcation lesions. Nine of them were located in the upstream part of the lesion (p=0.267).

### IVUS-VH findings in bifurcation as compared to non-bifurcation lesions

Vessel CSA was larger in bifurcation lesions as compared to non-bifurcations lesions (16.03±5.02 mm<sup>2</sup> vs. 14.63±5.57 mm<sup>2</sup>, p=0.006). Lumen and plaque cross-sectional areas were also larger in bifurcation lesions as compared to non-bifurcations lesions (7.14±3.35 mm<sup>2</sup> vs. 6.49±2.66 mm<sup>2</sup>, p=0.02 and 8.89±2.67 mm<sup>2</sup> vs. 8.14±3.13 mm<sup>2</sup>, p=0.007, respectively). Plaque burden in bifurcation lesions was 56.60±5.79% vs. 55.50±4.54%, p=0.04. Overall mean necrotic core area was larger in bifurcation lesions 0.84±0.55 mm<sup>2</sup> vs. 0.70±0.49 mm<sup>2</sup>, p=0.048. Adjusted for plaque size, mean percentage necrotic core was 15.48±8.02% vs. 14.51±7.64%, p=0.37. There was a trend towards a greater content of necrotic core in contact with the lumen in bifurcation

**Table 2. Geometrical and compositional analysis of bifurcation lesions.**

n=90	Downstream	MLA	Upstream	p*	p**
Vessel CSA (mm <sup>2</sup> )	14.66 (4.65)	14.45 (4.47)	16.93 (6.06)	<0.001	<0.001
Lumen CSA (mm <sup>2</sup> )	6.37 (2.56)	5.00 (1.81)	7.56 (4.60)	<0.001	<0.001
Plaque CSA (mm <sup>2</sup> )	8.29 (2.71)	9.45 (3.59)	9.37 (3.06)	<0.001	<0.001
Plaque burden (%)	56.91 (5.68)	64.44 (8.62)	56.83 (7.83)	0.928	<0.001
Necrotic core area (mm <sup>2</sup> )	0.75 (0.54)	0.96 (0.88)	0.89 (0.66)	0.013	0.014
Necrotic core (%)	15.58 (9.56)	15.62 (9.92)	15.32 (8.38)	0.982	0.905
Fibrous area (mm <sup>2</sup> )	2.95 (1.52)	3.69 (2.11)	3.48 (1.70)	<0.001	<0.001
Fibrous (%)	57.49 (11.85)	57.75 (11.66)	57.72 (9.30)	0.755	0.531
Fibrofatty area (mm <sup>2</sup> )	0.98 (0.96)	1.17 (1.07)	1.12 (0.98)	0.016	0.008
Fibrofatty (%)	17.87 (13.29)	17.69 (13.23)	17.36 (11.66)	0.858	0.475
Dense calcium area (mm <sup>2</sup> )	0.41 (0.36)	0.46 (0.43)	0.52 (0.41)	0.013	0.044
Dense calcium (%)	9.07 (8.33)	8.94 (9.36)	9.56 (7.67)	0.325	0.235
NCCL NC (%)	37.08 (21.04)	32.03 (26.67)	34.14 (16.67)	0.066	0.007
NCCL TP (%)	6.52 (6.46)	5.55 (6.70)	5.96 (5.58)	0.278	0.012
Major confluent NCCL TP (%)	4.57 (5.74)	3.69 (5.90)	3.87 (4.91)	0.070	0.001
Frames >10% major Confluent NCCL TP (%)	12.31 (23.95)	11.11 (31.60)	10.47 (19.24)	0.129	0.002

All parameters are means and standard deviation. \* Comparisons between downstream and upstream were made by Wilcoxon and McNemar tests.

\*\*Comparisons between the three were made by Friedman test. CSA: cross-sectional area; NC: necrotic core; TP: total plaque; NCCL: necrotic core in contact with the lumen

**Table 3. Geometrical and compositional analysis of non-bifurcation lesions.**

n=90	Downstream	MLA	Upstream	p*	p**
Vessel CSA (mm <sup>2</sup> )	14.44 (6.02)	14.23 (5.93)	14.96 (5.91)	0.056	0.011
Lumen CSA (mm <sup>2</sup> )	6.42 (2.78)	5.57 (2.66)	6.60 (2.86)	0.057	<0.001
Plaque CSA (mm <sup>2</sup> )	8.02 (3.45)	8.66 (3.98)	8.36 (3.33)	0.071	0.002
Plaque burden (%)	55.36 (4.42)	60.41 (7.62)	55.77 (5.26)	0.624	<0.001
Necrotic core area (mm <sup>2</sup> )	0.67 (0.52)	0.81 (0.76)	0.73 (0.55)	0.207	0.220
Necrotic core (%)	14.38 (7.96)	14.59 (9.28)	14.51 (8.23)	0.941	0.745
Fibrous area (mm <sup>2</sup> )	2.96 (1.94)	3.39 (2.35)	3.09 (1.87)	0.153	<0.001
Fibrous (%)	61.61 (10.92)	61.34(12.696)	60.71 (11.34)	0.367	0.745
Fibrofatty area (mm <sup>2</sup> )	0.77 (0.76)	0.85 (0.84)	0.82 (0.76)	0.142	0.068
Fibrofatty (%)	15.18 (10.60)	15.31 (11.34)	15.55 (10.38)	0.250	0.376
Dense calcium area (mm <sup>2</sup> )	0.38 (.39)	0.43 (0.45)	0.04 (0.39)	0.526	0.748
Dense calcium (%)	8.83 (8.04)	8.75 (8.56)	9.23 (8.49)	0.767	0.442
NCCL NC (%)	38.29 (22.49)	36.50 (27.64)	39.76 (19.86)	0.456	0.485
NCCL TP(%)	6.09 (5.55)	6.36 (8.23)	6.47 (5.69)	0.424	0.138
Major confluent NCCL TP (%)	3.82 (4.92)	3.81 (5.86)	3.79 (4.27)	0.642	0.039
Frames >10% major confluent NCCL TP (%)	9.93 (25.13)	9.47 (29.45)	8.55 (20.40)	0.864	0.105

All parameters are means and standard deviation. \* Comparisons between downstream and upstream were made by Wilcoxon and McNemar tests.

\*\* Comparisons between the three were made by Friedman test. CSA: cross-sectional area; NC: necrotic core; TP: total plaque; NCCL: necrotic core in contact with the lumen

lesions. The mean proportion of frames with MCNC >10% in bifurcation lesions was 11.68±17.18 vs. 8.95±17.86 in non-bifurcation lesions, p=0.065. This resulted in a statistically significant difference in the frequency of ID-TCFAs between bifurcation lesions 20 vs. 13, p=0.03 (Table 4)

**Table 4. Geometrical and compositional analysis of non-bifurcation and bifurcation lesions.**

	Non-bifurcation lesions	Bifurcation lesions	p
Length (mm)	9.84 (9.65)	14.62 (14.24)	0.003
Vessel CSA (mm <sup>2</sup> )	14.63 (5.57)	16.03 (5.02)	0.006
Lumen CSA (mm <sup>2</sup> )	6.49 (2.66)	7.14 (3.35)	0.020
Plaque area (mm <sup>2</sup> )	8.14 (3.13)	8.89 (2.67)	0.007
Plaque burden (%)	55.50 (4.54)	56.60 (5.79)	0.040
Necrotic core area (mm <sup>2</sup> )	0.70 (0.49)	0.84 (0.55)	0.048
Necrotic core (%)	14.51 (7.64)	15.48 (8.02)	0.372
Fibrous area (mm <sup>2</sup> )	3.02 (1.72)	3.24 (1.45)	0.057
Fibrous (%)	61.65 (10.32)	58.26 (9.08)	0.002
Fibrofatty area (mm <sup>2</sup> )	0.77 (0.70)	1.00 (0.86)	0.027
Fibrofatty (%)	15.02 (9.16)	16.95 (11.12)	0.273
Dense calcium area (mm <sup>2</sup> )	0.39 (0.34)	0.49 (0.36)	0.022
Dense calcium (%)	8.82 (7.59)	9.31 (6.92)	0.310
NCCL NC (%)	39.67 (17.92)	36.05 (15.92)	0.074
NCCL TP (%)	6.23 (4.95)	6.39 (4.96)	0.716
Major confluent NCCL TP (%)	3.71 (3.70)	4.18 (4.07)	0.555
Frames > 10% Major Confluent NCCL TP (%)	8.95 (17.86)	11.68 (17.18)	0.065

All parameters are in means (SD). CSA: Cross-sectional area; NCCL NC (%): percentage of necrotic core in contact with the lumen of the necrotic core area; NCCL TP: percentage of necrotic core in contact with the lumen of the total plaque area

## Discussion

The main findings of this study were the following: (i) In bifurcation and non-bifurcation lesions there are no significant difference in compositional analyses between upstream and downstream segments; (ii) Bifurcation lesions have a significantly larger plaque burden and a larger area of necrotic core in contact with the lumen. (iii) This resulted in a greater number of IDTCFAs in bifurcation versus non-bifurcation lesions.

In general the content of necrotic core and plaque composition was comparable between upstream and downstream segments in bifurcation and non-bifurcation lesions. These results are in line with our previous findings which demonstrated that plaque rupture was present in 39.3% of upstream plaque, 21.4% of plaque at the MLA and 32.1% of downstream plaque.<sup>5</sup>

Important geometrical differences have been found between the non-obstructive bifurcation and non-bifurcation lesions evaluated in this study. Notably lesion length varied significantly between lesions (14.6 mm bifurcation vs. 9.8 mm non-bifurcation), and consequently the upstream and downstream segment lengths were different – the upstream segment was almost twice as long in bifurcation lesions (9.09 vs. 5.47 mm), with only a 1.1% absolute difference in %plaque burden (1.9% relative difference); this suggests a very different geometry in bifurcation and non-bifurcation lesions. With such a marked difference in lesion geometry, and by association, shear stress, one would expect a greater difference in plaque composition between lesion types. Some reports have suggested that shear stress may play a role in both the distribution of the plaque, and the distribution of components within the plaque.<sup>6</sup> The geometry of an encroaching atherosclerotic plaque has an impact on the pattern of the blood flow. Indeed, proximal to the MLA i.e., at upstream endothelium



sites the plaque is under high-shear stress, whereas at downstream sites low-shear stress prevails. Furthermore, atherosclerotic plaque composition varies greatly,<sup>7</sup> with a higher concentration of macrophages upstream, whilst smooth muscle cells (SMCs) predominate in the downstream part of the atherosclerotic plaque.<sup>7,8</sup> At present there is no overall consensus on the role of shear stress on either plaque composition or, as a trigger factor for plaque rupture. Further investigation is warranted.

To the best of our knowledge, this is the first *in vivo* study comparing geometrical and compositional analyses in bifurcation and non-bifurcation lesions. Bifurcation lesions account for approximately a quarter of lesions undergoing PCI, and have consistently been associated with poorer outcomes when compared to non-bifurcation lesions, although the reasons behind this are not entirely apparent.<sup>9,10</sup> Previously the use of two stents was blamed, however data continues to indicate that poorer outcomes persist even in patients treated with one-stent strategies. Tsuchida et al reported a MACCE rate of 14.1% in patients with bifurcation lesions treated with one-stent compared to 11.0% in patients without bifurcation lesions.<sup>11</sup> Other possible causes for these poorer outcomes include the plaque burden at bifurcations sites, which may consequently influence restenosis as has been demonstrated in patients with diabetes. Diabetes not only results in a greater plaque burden,<sup>12</sup> but has also consistently been identified as an independent predictor of restenosis after PCI with either bare metal or drug eluting stents.<sup>13,14</sup> Another possibility is that the restenosis is related to the composition of the underlying plaque. Previously in carotid arteries Hellings et al demonstrated a positive correlation between plaque composition and rates of restenosis after stenting.<sup>15</sup>

Two studies have evaluated the usefulness of IVUS-VH plaque composition to predict the risk of embolisation during stenting<sup>16,17</sup> In one of these studies Kawamoto et al used a Doppler guidewire in 44 patients undergoing elective PCI to record the high-intensity transient signals (HITS) produced by the small embolic particles that were liberated during stenting. Patients were then divided into the tertiles according to the HITS counts. Dense calcium and necrotic core area were significantly larger in the highest tertile. Moreover, in the multivariate logistic regression analysis, only necrotic core area was an independent predictor of a high HITS counts (odds ratio 4.41,  $p=0.045$ ). The greater plaque burden and percentage of necrotic core seen in bifurcation lesions may therefore account for the increased risk of periprocedural MI during treatment of bifurcation lesions.<sup>10</sup> Moreover, the use of plaque stabilising medication such as statins may reduce this risk, as suggested by the recent ARMYDA-RECAPTURE study which demonstrated, albeit not specifically in bifurcation lesions, a reduction in periprocedural myocardial infarction ( $p=0.056$ ) following the reloading of patients with 80 mg of atorvastatin.<sup>18</sup>

### Limitations of the study

There are a number of limitations associated with the present study. Firstly, no imaging was performed in the side branch of the bifurcation lesion. Moreover, we acknowledge that there was no independence between the observations, such that bifurcation and non-bifurcation lesions may have come from the same patient.

These observations are only related to non-obstructive lesions; the size and composition may be different in obstructive plaques. The number of high-risk plaques (i.e., TCFA) is low and although their geographic spread is reported here, no definitive conclusions can be drawn on this, primarily because this study does not represent the whole spectrum of the disease.

### Conclusions

Bifurcation lesions appear to have a large plaque burden and different plaque composition compared to non-bifurcation lesions, and this may partly explain the adverse outcomes seen following treatment of bifurcation lesions in contemporary practice.

### Acknowledgements

Funding/Support: This study was funded by Volcano Corporation.

Role of the Sponsor: The sponsor participated in discussions regarding study design and protocol development and provided logistical support during the trial.

Database was performed by a contract research organisation, Pacific Data Design, California, US, under contract to the sponsor.

### VOLCANO REGISTRY Investigators and participating centres:

United States: Jason Rogers, MD, UC Davis Medical Center, Sacramento, CA; Steve Marso, MD, Mid-America, Kansas City, MO; Jim Margolis, MD, Miami Heart, Miami, FL; Amir Lerman, MD, Mayo Clinic, Minneapolis, MN; Juan Pittaluga, MD, Winchester Medical, Winchester, VA; George Revtyak, MD, St. Francis Hospital, Beech Grove, IN; Ed O'Leary, MD, Nebraska Heart, Omaha, NE; Murat Tuzcu, MD, Cleveland Clinic Foundation, Cleveland, OH; Nabil Dib, MD, Arizona Heart, Phoenix, AZ; Rajesh Dave, MD, Pinnacle Health Harrisburg, PA; Morton Kern, MD, Saint Louis University, Saint Louis, MO; John Hodgson, MD, Saint Joseph's Hospital, Phoenix, AZ; Samer Kazziha, MD, Mount Clemens General, Mt. Clemens, MI; Greg Braden, MD, Forsyth Hospital, Forsyth, NC; Louis I. Heller, MD, Saint Joseph's Hospital, Atlanta, GA; Marty Leon, MD, Columbia University Medical Center, New York, NY; Joseph Puma, MD, New York Methodist, Brooklyn, NY.

Europe: V. Klaus, MD, Innenstadt, Munich, Germany; M. Pieper, MD, Herz-und Neurozentrum, Kreuzlingen, Switzerland; D. Glogar, MD, AKH, Vienna, Austria; P. Oemrawsingh, MD, LUMC, Leiden, The Netherlands; O. Bleie, MD, Haukeland Hospital, Bergen, Norway; D. Dudek, MD, Jagiellonian University, Krakow, Poland; Schiele, MD, CHU, Besancon, France; M. Sabate, MD, Hospital Clinico San Carlos, Madrid, Spain; Prof. P. Serruys, MD, Thoraxcenter, Rotterdam, The Netherlands; R. Erbel, MD, Westdeutsches Herzzentrum, Essen, Germany; W. Wijns, MD, OLVZ, Aalst, Belgium; Colman, MD, Valdecilla Hospital, Santander, Spain; F. Prati, MD, San Giovanni, Roma, Italy; P. Sganzerla, MD, Cliniche Gavazzeni, Bergamo, Italy; P. Presbitero, MD, Clinica Humanitas, Rozzano, Italy; Miller, MD, Ichilov, Tel Aviv, Israel; R. Kornowski, MD, Rabin Medical Center; Petah Tiqwa, Israel; A. Iniguez, MD, Meixoeiro, Vigo, Spain; E. Eeckhout, MD, CHUV, Lausanne, Switzerland; Harnek, MD, University Hospital, Lund, Sweden; Quinha, MD, Hospital de Santa Marta, Lisbon, Portugal.

Japan: Osamu Kato, MD, Kenya Nasu, MD, Takahiko Suzuki, Toyohashi Heart Center, Toyohashi; Satoru Sumitsuji, MD, Rinku

General Medical Center, Izumisano; Satoshi Saito, MD, Junko Honye, MD, Nihon University, Tokyo.

## References

1. Virmani R, Burke AP, Farb A, Kolodgie FD. Pathology of the vulnerable plaque. *J Am Coll Cardiol*. 2006;47:C13-18.
2. Gonzalo N, Garcia-Garcia HM, Regar E, Barlis P, Wentzel J, Onuma Y, Ligthart J, Serruys PW. In vivo assessment of high-risk coronary plaques at bifurcations with combined intravascular ultrasound and optical coherence tomography. *JACC Cardiovasc Imaging*. 2009;2:473-482.
3. Garcia-Garcia HM, Goedhart D, Schuurbijs JC, Kukreja N, Tanimoto S, Daemen J, Morel MA, Bressers M, van Es GA, Wentzel J, Gijssen F, van der Steen AF, Serruys PW. Virtual histology and remodeling index allow in vivo identification of allegedly high risk coronary plaques in patients with acute coronary syndromes: a three vessel intravascular ultrasound radiofrequency data analysis. *EuroIntervention*. 2006;2:338-344.
4. Sawada T, Shite J, Garcia-Garcia HM, Shinke T, Watanabe S, Otake H, Matsumoto D, Tanino Y, Ogasawara D, Kawamori H, Kato H, Miyoshi N, Yokoyama M, Serruys PW, Hirata K. Feasibility of combined use of intravascular ultrasound radiofrequency data analysis and optical coherence tomography for detecting thin-cap fibroatheroma. *Eur Heart J*. 2008;29:1136-1146.
5. Rodriguez-Granillo GA, Garcia-Garcia HM, Valgimigli M, Vaina S, van Mieghem C, van Geuns RJ, van der Ent M, Regar E, de Jaegere P, van der Giessen W, de Feyter P, Serruys PW. Global characterization of coronary plaque rupture phenotype using three-vessel intravascular ultrasound radiofrequency data analysis. *Eur Heart J*. 2006.
6. Zarins CK, Bomberger RA, Glagov S. Local effects of stenoses: increased flow velocity inhibits atherogenesis. *Circulation*. 1981;64:11221-227.
7. Krams R, Verheye S, van Damme LC, Tempel D, Gourabi BM, Boersma E, Kockx MM, Knaapen MW, Strijder C, van Langenhove G, Pasterkamp G, van der Steen AF, Serruys PW. In vivo temperature heterogeneity is associated with plaque regions of increased MMP-9 activity. *Eur Heart J*. 2005;26:2200-2205.
8. Dirksen MT, van der Wal AC, van den Berg FM, van der Loos CM, Becker AE. Distribution of inflammatory cells in atherosclerotic plaques relates to the direction of flow. *Circulation*. 1998;98:2000-2003.
9. Serruys PW, Ong ATL, Morice MC, De Bruyne B, Colombo A, Macaya C, Richardt G, Fajadet J, Hamm C, Dawkins K. Arterial Revascularisation Therapies Study Part II- Sirolimus-eluting stents for the treatment of patients with multivessel de novo coronary artery lesions. *EuroIntervention*. 2005;1:147-156.
10. Garg S. The outcome of bifurcation lesion stenting using a biolimus eluting stent with a biodegradable polymer compared to a sirolimus eluting stent with a durable polymer. Presentation EuroPCR, 20th May 2009. Online [www.europcronline.com/fo/lecture/view\\_slide.php?idCongres=5&id=7856](http://www.europcronline.com/fo/lecture/view_slide.php?idCongres=5&id=7856). Accessed July 14th 2009.
11. Tsuchida K, Colombo A, Lefevre T, Oldroyd KG, Guetta V, Guagliumi G, von Scheidt W, Ruzyllo W, Hamm CW, Bressers M, Stoll HP, Wittebols K, Donohoe DJ, Serruys PW. The clinical outcome of percutaneous treatment of bifurcation lesions in multivessel coronary artery disease with the sirolimus-eluting stent: insights from the Arterial Revascularization Therapies Study part II (ARTS II). *Eur Heart J*. 2007;28:433-442.
12. Nicholls SJ, Tuzcu EM, Kalidindi S, Wolski K, Moon KW, Sipahi I, Schoenhagen P, Nissen SE. Effect of diabetes on progression of coronary atherosclerosis and arterial remodeling: a pooled analysis of 5 intravascular ultrasound trials. *J Am Coll Cardiol*. 2008;52:255-262.
13. Kastrati A, Dibra A, Mehilli J, Mayer S, Piniack S, Pache J, Dirschinger J, Schomig A. Predictive factors of restenosis after coronary implantation of sirolimus- or paclitaxel-eluting stents. *Circulation*. 2006;113:2293-2300.
14. Kastrati A, Schomig A, Elezi S, Schuhlen H, Dirschinger J, Hadamitzky M, Wehinger A, Hausleiter J, Walter H, Neumann FJ. Predictive factors of restenosis after coronary stent placement. *J Am Coll Cardiol*. 1997;30:1428-1436.
15. Hellings WE, Moll FL, De Vries JP, Ackerstaff RG, Seldenrijk KA, Met R, Velema E, Derksen WJ, De Kleijn DP, Pasterkamp G. Atherosclerotic plaque composition and occurrence of restenosis after carotid endarterectomy. *JAMA*. 2008;299:547-554.
16. Kawaguchi R, Oshima S, Jingu M, Tsurugaya H, Toyama T, Hoshizaki H, Taniguchi K. Usefulness of virtual histology intravascular ultrasound to predict distal embolization for ST-segment elevation myocardial infarction. *J Am Coll Cardiol*. 2007;50:1641-1646.
17. Kawamoto T, Okura H, Koyama Y, Toda I, Taguchi H, Tamita K, Yamamuro A, Yoshimura Y, Neishi Y, Toyota E, Yoshida K. The relationship between coronary plaque characteristics and small embolic particles during coronary stent implantation. *J Am Coll Cardiol*. 2007;50:1635-1640.
18. Di Sciascio G, Patti G, Pasceri V, Gaspardone A, Colonna G, Montinaro A. Efficacy of atorvastatin reload in patients on chronic statin therapy undergoing percutaneous coronary intervention: results of the ARMYDA-RECAPTURE (Atorvastatin for Reduction of Myocardial Damage During Angioplasty) Randomized Trial. *J Am Coll Cardiol*. 2009;54:558-565.